



This discussion paper is/has been under review for the journal Natural Hazards and Earth System Sciences (NHESD). Please refer to the corresponding final paper in NHESD if available.

# Geomorphological surveys and software simulations for rock fall hazard assessment: a case study in the Italian Alps

S. Devoto, C. Boccali, and F. Podda

Dipartimento di Matematica e Geoscienze, Università degli Studi di Trieste, Via Weiss, 2, Trieste, 34128, Italy

Received: 29 October 2014 – Accepted: 17 November 2014 – Published: 5 December 2014

Correspondence to: S. Devoto (sdevoto@units.it)

Published by Copernicus Publications on behalf of the European Geosciences Union.

**NHESD**

2, 7329–7365, 2014

## A case study in the Italian Alps

S. Devoto et al.

Title Page

Abstract

Introduction

Conclusions

References

Tables

Figures



Back

Close

Full Screen / Esc

Printer-friendly Version

Interactive Discussion



## Abstract

In northern Italy, fast-moving landslides represent a significant threat to the population and human facilities. In the eastern portion of the Italian Alps, rock falls are recurrent and are often responsible for casualties or severe damage to roads and buildings. The above-cited type of landslide is frequent in mountain ranges, is characterised by strong relief energy and is triggered by earthquakes or copious rainfall, which often exceed 2000 mm yr<sup>-1</sup>. These factors cause morphological dynamics with intense slope erosion and degradation processes.

This work investigates the appraisal of the rock-fall hazard related to the presence of several large unstable blocks located at the top of a limestone peak, approximately 500 m NW with respect to the Village of Cimolais.

Field surveys recognised a limestone block exceeding a volume of 400 m<sup>3</sup> and identified this block as the most hazardous for Cimolais Village because of its proximity to the rocky cliff.

A first assessment of the possible transit and stop areas has been investigated through in-depth traditional activities, such as geomorphological mapping and aerial photo analysis. The output of field surveys was a detailed land use map, which provided a fundamental starting point for rock fall software analysis. The geomorphological observations were correlated with DTMs derived by regional topography and Airborne Laser Scanning (ALS) surveys to recognise possible rock fall routes.

To simulate properly rock fall trajectories with a hybrid computer program, particular attention was devoted to the correct quantification of rates of input parameters, such as restitution coefficients and horizontal acceleration associated to earthquakes, which historically occur in this portion of Italy.

The simulation outputs regarding the distribution of rock fall end points and kinetic energy along rock falling paths highlight the hazardous situation for Cimolais Village. Because of this reason, mitigation works have been suggested to immediately reduce the landslide risk. This proposal accounts for the high volume of blocks, which, in case

# NHESSD

2, 7329–7365, 2014

## A case study in the Italian Alps

S. Devoto et al.

Title Page

Abstract

Introduction

Conclusions

References

Tables

Figures



Back

Close

Full Screen / Esc

Printer-friendly Version

Interactive Discussion



of a fall, render the passive mitigation measures already in place at the back of Cimolais worthless.

## 1 Introduction

Concerning Alpine slope-failure phenomena, the detachment and fall of rocky blocks from steep slopes represent more than 40 % of landslides (Cocco, 1993). Rock falls, because of their very fast speed (Cruden and Varnes, 1996), often lead to catastrophic consequences that cause human casualties or severe damages to buildings and roads (Agliardi et al., 2009; Mignelli et al., 2014). To assess rock fall hazards using software analysis, field geomorphological observations are crucial to recognise accurately the source areas of rock falling phenomena (Parise, 2002), to quantify the volumes of unstable blocks and to identify the possible block trajectories along the underlying transit areas (Del Maschio et al., 2007).

This work investigates a case study situated in the eastern portion of the Italian Alps, in which rock falls are recurrent and problematic (Guzzetti, 2000; Tagliavini et al., 2009). These rock falls are related to the presence of steep cliffs (Valagussa et al., 2014) that are often weakened by the presence of persistent discontinuities originated by faults. A limestone slab is located at the top of a calcareous peak named Crep Savath and overhangs the Cimolais Village. This slab is intensely jointed and is characterised by the presence of several boulders, which generates a high rock fall hazard to underlying human facilities. The elevation and constant steepness of debris cones at the bottom of Crep Savath rocky slopes, combined with the scarce presence of ledges and the poor high-forest vegetation, suggest that rock falls can directly reach the northern sector of the Cimolais Village, causing possible casualties or serious damage to human facilities. Particular attention was devoted to recognising geomorphological features related to the rock fall phenomena and then through simulations to identify portions of the terrain subjected to landslides.

### A case study in the Italian Alps

S. Devoto et al.

Title Page

Abstract

Introduction

Conclusions

References

Tables

Figures

◀

▶

◀

▶

Back

Close

Full Screen / Esc

Printer-friendly Version

Interactive Discussion



## A case study in the Italian Alps

S. Devoto et al.

Title Page

Abstract

Introduction

Conclusions

References

Tables

Figures

◀

▶

◀

▶

Back

Close

Full Screen / Esc

Printer-friendly Version

Interactive Discussion



In engineering geology practice, these studies are mainly performed along specific slope profiles (Crosta and Agliardi, 2003). We simulated rock fall trajectories using a 2-D software analysis along two paths that were derived from a topographic map and ALS-derived DTM. The simulation outputs outlined for the simulated blocks the fall paths, the potential run-out zones, the envelopes of trajectories and the velocity and energy distribution along these paths. These results are crucial for rock fall hazard assessment and for assist regional authorities in planning strategies for landslide risk reduction. The outcomes achieved permit the identification of vulnerable elements, which could be affected by landslides, and the assessment of their associated risk (Cavallin et al., 2011) for buildings in Cimolais.

## 2 The study area

The Crep Savath Mountain and the Village of Cimolais are located in the eastern Dolomites, which are included in the “Southern Alps”. Dolomites were recently included in the World Heritage List for their peculiar geomorphological landforms (Panizza, 2011).

As reported by Dykes et al. (2013), numerous landslides affect the mountainous region of northeast Italy and their types and characteristics are strongly related to the geology and the geomorphology, particularly with respect to structural controls.

The landscape and geomorphological features of the study area present the typical landforms of the Dolomites: Crep Savath is a calcareous peak limited by steep slopes, which has abundant talus deposits at the foot and borders narrow valleys, which are occupied by meadows and small settlements.

The Crep Savath rock masses are situated NW with respect to the junction between the Cimoliana Stream and the National Road nr. 251, which connects the Vajont Valley to the Cimolais Village. The latter is located at the intersection of two valleys that are constituted mainly of alluvial deposits.

To the NW, the study area is bounded by Mont Lodina and is characterised by the presence of the Fesena Valley, which limits westerly the Crep Savath peak.

The geological map illustrates the lithology and the structural features of the study area (Fig. 1), which deeply influences the geomorphological landscape.

From a structural point of view, the study area presents a complex configuration, related to a polyphasic deformation (Carulli, 2006). The main tectonic lineament, which originated the actual structural landform of Crep Savath, is a low-angle reverse fault that is NW–SE oriented (see line A in Fig. 1). The above-mentioned fault caused the overthrust of the stratigraphic succession ranging from the Igne Formation to the Scaglia Rossa Formation (Riva et al., 1990).

The Scaglia Rossa Formation is constituted by marly limestone or reddish marls characterised by no evident stratification. Conversely, dark or light cherty dolomites are dominant in the Soverzene Formation.

The overthrusting succession during the movement was folded and reversed forming a lying anticline, of which only the reversed flank can be observed.

Vajont Formation consists of a massive and resistant limestone and constitutes the Crep Savath peak, including overlying unstable blocks. The blocks are separated mainly by two discontinuity sets: a series of cuts, sub-horizontal or NE slightly tilted, which interest the fold hinge and formed these high rock pillars (see Block 1 in Fig. 2), and sub-vertical faults oriented approximately NE–SW. The sub-vertical faults were originated by compressive stresses related to the high compressive structural setting and act like slide rails for the blocks. For these reasons, the top of Crep Savath houses an intense landsliding activity: the detachment and fall of debris or rocks are recurrent. Specifically rock fall phenomena mainly affect the southern and western portions of Crep Savath, whereas rock topples evolve to falls along the eastern sector. Extensive talus cones, generated by fallen and rebound motions of debris and blocks, show these intense slope-failure activities. The landslide **accumulations** are limited westerly by the Fesena Valley and southerly by the road, which separates the northern part of Cimolais and the slope-failure cone.

**A case study in the Italian Alps**

S. Devoto et al.

Title Page

Abstract

Introduction

Conclusions

References

Tables

Figures

◀

▶

◀

▶

Back

Close

Full Screen / Esc

Printer-friendly Version

Interactive Discussion



Excluding some central areas, the landslide accumulations consist of a mix of gravel, pebbles and angular fragments of rocks, covered mostly by shrub vegetation, which frequently exhibits traces of transit or stop motions of the rocky blocks coming from the overhanging summit of the Crep Savath slab.

### 3 Rock fall source area

To investigate rock fall phenomena, traditional surveys are crucial (Piacentini et al., 2013; Salvini et al., 2011). Field investigations were performed on the summit of the Crep Savath peak and along the underlying scree slopes located at the bottom of the limestone rock masses. Aerial-photo interpretation accompanied geomorphological surveys to identify possible unstable blocks and their position with respect to the structural escarpments, which limit the limestone slab. The outputs of these investigations recognised 13 limestone blocks (Fig. 2). The latter were originated by the fragile behaviour of the Vajont Formation, deeply jointed by the presence of regional faults, as illustrated previously in the geological section of Fig. 1c.

The volumes of blocks, directions of block trajectories and their rock fall susceptibilities are listed in Table 1. Block volumes are determined by field scan lines. Conversely, rock fall susceptibilities were examined according to the position of each block with respect to the slope cliffs and the properties of discontinuities. These fissures often partially isolate the investigated unstable blocks from the Crep Savath slab.

Five boulders are located at 996 m.a.s.l. and include Block 1, which can be considered the most hazardous in the entire study area. The hazard is related to the large volume, the position close to the easterly structural escarpment and the poor properties of a persistent joint. This discontinuity partially separates Block 1 from backyard intact rock masses. The hazardous position of Block 1 is known by locals and is witnessed by oral tradition: the stability of this block is related to an invisible wire connected to the Cimolais church steeple and created by an old witch.

## A case study in the Italian Alps

S. Devoto et al.

Title Page

Abstract

Introduction

Conclusions

References

Tables

Figures

◀

▶

◀

▶

Back

Close

Full Screen / Esc


Printer-friendly Version

Interactive Discussion



The above-cited block is clearly visible by the village because of its vertical predominant orientation and large dimensions: 14 m in height, 6 m wide and 5 m in length (Fig. 2a). The estimated volume exceeds the 400 m<sup>3</sup>.

A sub-vertical opened joint partially filled by debris separates Block 1 from Blocks 2, 3, 4 and 5, as shown in Fig. 2c. The blocks are isolated each other by two discontinuity sets oriented approximately 250/60 and 85/75. Given the position of these blocks, which completely lean on Block 1, their stability conditions are precarious. For a Block 1 collapse event ~~from structural escarpment~~, the stability conditions of the four blocks would be compromised with a subsequent falling motion along the identical trajectory of Block 1.

On the western portion of the Crep Savath slab, at 1010 m a.s.l., we identified eight potentially unstable limestone boulders, listed in Table 1. Field observations and aerial-photo interpretation suggest a possible direction of slope-failure movement towards the Fesena Valley, which is not populated. In particular, Block 9 shows an irregular shape and rests on an unstable sheet. Additionally, trees, which increase stability conditions, surround Block 12 and 13. 

The presence of abundant debris and small boulders (around the cubic meter) in the eastern portion of Fesena Valley confirms the intense landsliding activities related to the occurrence of rock falls detached by western Crep Savath cliffs.

## 4 Rainfall and earthquake analysis

### 4.1 Climate

The climate of the eastern Italian Alps is classified as moderately cold (class D of Köppen classification, Köppen, 1931). The mean annual temperature is 5 °C. Spring and autumn are moderately cold and winter mean values are just below 0 °C along the valley bottom (Marcato et al., 2006).

## A case study in the Italian Alps

S. Devoto et al.

Title Page

Abstract

Introduction

Conclusions

References

Tables

Figures



Back

Close

Full Screen / Esc

Printer-friendly Version

Interactive Discussion



## A case study in the Italian Alps

S. Devoto et al.

Title Page	
Abstract	Introduction
Conclusions	References
Tables	Figures
◀	▶
◀	▶
Back	Close
Full Screen / Esc	
Printer-friendly Version	
Interactive Discussion	



An analysis of historical data shows that in the Eastern sector of Italian Alps rainfalls are abundant in November, October and in the late spring. In particular, late autumn precipitations often trigger hydrological and flood disasters, which usually hit the Friuli-Venezia Giulia Region as already reported by Paronuzzi (2006).

Rainfall data have been collected and analysed from two rain gauges that are located one in Cimolais, along the National Road nr. 251, and the other in Barcis Village, approximately 14 km SE of the study area. As shown in Fig. 3, annual rainfall is extremely abundant, exceeding the average quantity recorded in the central sector of the Dolomites (Fazzini, 2005), which corresponds approximately to 1000 mm year<sup>-1</sup>. Secondly, significant variations in excess of 2000 mm year<sup>-1</sup> are noted.

Taking the example of one of the rainiest years (2000; Fig. 4), the rainy periods are noted to span between September to the end of November.

The major peak was recorded between October and November when 100 mm of daily precipitation amounts were reached. The peak at the end of March was caused by snow precipitation.

### 4.2 Earthquakes

The NW sector of the Friuli Venezia Giulia Region, in which the village of Cimolais is located, is characterised by high-seismic activities (Chiarabba et al., 2005). In fact, the study area lies entirely in a sector classified as a high seismic zone, accounting for both national and regional laws.

The seismic dataset relating to historical earthquakes and the inventories related to recent events were collected and analysed. The outcomes indicate the majority of earthquakes were superficial events.

### 4.3 Historical analysis of rainfalls and earthquakes as triggering mechanisms

According to several studies (Wieczorek and Jäger, 1996; Crosta, 1998; Krautblatter and Moser, 2009), rainfalls and earthquakes are the main triggering factors of rock



fall events in mountainous areas. Moreover, the alternation of freezing and thawing of infiltrated water plays a crucial role in the enlargement of fissures (Matsuoka and Sakai, 1999). The combination of these mechanisms addresses the timing and the frequency of rock falls (Flageollet and Weber, 1996).

5 McCauley et al. (1985) identify rainfalls as primarily responsible for the collapse events, as reported in a study conducted on Yosemite National Park (California). This result is supported by data analysed for 395 historical slope-failure events. Rain storms (26.6%) dominate the other recognised triggering factors, such as rapid snowmelt (8.1%) or earthquakes (5.3%). Conversely, Wieczorek and Jäger (1996) found that  
10 earthquakes are responsible for a greater cumulative volume than these other predisposing factors.

In recent years, many models were introduced to identify the correlation between these triggering phenomena and the activation threshold of rock fall, notably in terms of predicting and mitigating landslide hazards.

### 15 4.3.1 Rainfalls

According to Paronuzzi (2006) in the NE Italian Alps, intense rains distributed within 24–48 h trigger landslide phenomena. A more detailed study performed by Paronuzzi and Gnech (2007) based on analysis of a sample of 69 rock falls that occurred in the Friuli Venezia Giulia Region, provides a first indication about the amount of rainfall that can trigger rock fall events. The study outcomes show that daily rainfall exceeding 10 mm can be considered critical for the stability of blocks whose volumes do not exceed 500 m<sup>3</sup>. The critical rain events ( $P \geq 10 \text{ mm day}^{-1}$ ) have a relatively high frequency, notably in the 5 days prior to the collapse, and often correspond to episodes of low cumulative rain (10–100 mm) and of moderate hourly intensity (5–25 mm h<sup>-1</sup>). This  
20 research also noted that the time interval between the critical rainfall and the moment of rupture varies depending on the conditions of the system supply and on the properties of the discontinuity sets such as aperture and persistence (Paronuzzi and Gnech, 2007).  
25

## A case study in the Italian Alps

S. Devoto et al.

Title Page

Abstract

Introduction

Conclusions

References

Tables

Figures

◀

▶

◀

▶

Back

Close

Full Screen / Esc

Printer-friendly Version

Interactive Discussion



## A case study in the Italian Alps

S. Devoto et al.

Title Page

Abstract

Introduction

Conclusions

References

Tables

Figures

◀

▶

◀

▶

Back

Close

Full Screen / Esc

Printer-friendly Version

Interactive Discussion



Processing information, obtained from a rain gauge installed in Cimolais Valley (Fig. 4), displayed that it rained more than  $10 \text{ mm day}^{-1}$  for 48 days, more than  $50 \text{ mm day}^{-1}$  for 15 days and more than  $100 \text{ mm day}^{-1}$  for 2 days in 2000. In many cases, the rainfall does not last only for one day, but normally the rainfall overruns several days, on average 3 to 6, with accumulated precipitation constantly greater than 50 mm.

In 2002, several researchers, partners of the AVI Project (powered by CNR) noted a landslide occurred on 6 November 2000 that forced the closing of a road. When we analyse in detail that period in the rainfall graph, we note that before the landslide more than 160 mm of rain had fallen in 6 days, agreeing with Paronuzzi and Gnech (2007).

The lack of an updated inventory of smaller collapse events in the study area hinders a more detailed comparison with the rainfall data; however, it is evident that severe rainfall events can be considered the main triggering factor for fast-moving landslides.

### 4.3.2 Earthquakes

Although rock falls are one of the main secondary effects of large earthquakes (Hack et al., 2007), the influence of seismic activity on landslides is less understood compared to rainfall-induced landslides. The effect of rain on the slope-failure processes is more easily determined than the contribution of ground motion related to earthquake acceleration. Although some recent improvements have occurred in earthquake prediction, forecasting epicentres and magnitudes of earthquake occurrences that may trigger landslides is still not possible (Sidle and Ochiai, 2006). At present, some of the useful information related to earthquake-induced landslides is derived from retrospective analyses of landslides occurring during periods with different magnitudes and conditions of ground motion (Jibson and Keefer, 1989; Duman et al., 2005). In a review of intensity reports from 300 earthquakes, Keefer (2002) determined that the lowest magnitude earthquake required to trigger rock falls or other fast-moving landslides is  $\approx 4.0$ . However, Keefer (1984) also supports that an earthquake with  $M \approx 4.0$  does not create an area likely to experience some degree of landsliding, except the area coin-

cided with the hypocentre. Conversely, for earthquakes with  $M = 5.4$  Keefer estimated an area of influence of  $250 \text{ km}^2$ ; when  $M = 9.2$ , a maximum area of  $500\,000 \text{ km}^2$ .

As reported by Wieczorek and Jäger (1996), the postponed effect of earthquake shaking in deeply jointed rock masses and accelerating the slope-failure rate in the months, years or decades following an earthquake could not be evaluated.

According to Keefer (1984, 2002), we analysed earthquakes with  $M > 5.4$  that were recorded historically within 250 km from Cimolais Village. Table 2 lists only the earthquakes occurring in the last three centuries (INGV, 2010).

The outputs of this desk research reveal the absence of reports or historical documents regarding landslides triggered by earthquakes listed in Table 2 nearby Cimolais Village and its surroundings. Conversely, the 1976 earthquakes, which hit NE Friuli, likely triggered several rock falls in NW Friuli, in which Cimolais Village lies. In particular, the 6 May 1976, earthquake was one of the strongest earthquakes in south-central Europe (Rogers and Cluff, 1979), reaching a 6.4 surface wave magnitude. The studies of the 1976 seismic-induced landslides concentrated around the epicentres of the two strongest shocks, as reported by Govi (1977) and Valagussa et al. (2014), on the effects and the areas subject to transit and arrest of fallen blocks (Martinis, 1977; Onofri and Candian, 1979). Given the deficiency of a historical inventory of landslides in the surroundings of Cimolais, a direct correlation between slope-failure phenomena and regional earthquakes is not evident but probable. In addition, the catalogue of the AVI project (powered by CNR) does not contain any event directly caused by an earthquake. Nevertheless, the weakening effects of earthquakes act as secondary triggering mechanisms, for which a condition of slope instability is present because of other predisposing factors such as the intense fracturing of rock masses, intense rainfalls, etc.



## A case study in the Italian Alps

S. Devoto et al.

Title Page

Abstract

Introduction

Conclusions

References

Tables

Figures



Back

Close

Full Screen / Esc

Printer-friendly Version

Interactive Discussion



## 5 Rock fall propagation modelling


### 5.1 Description of the method

The dynamics and the maximum distance reached by a falling block down a slope depends on a series of variable factors, such as the size, shape and rocky material of the block, the slope inclinations and the materials of the slope (Schweigl et al., 2003). Rock fall initiates with the detachment of rocks **from bedrock slopes**. Therefore, the block descends the underlying slope in different modes of motion. The types of motion strongly depend on the mean slope gradient, as illustrated in Fig. 5.

~~The three modes of block motions are free fall through the air, bouncing or rolling over the slope topography (Dorren, 2003).~~

Other factors, such as block speed, influence the type of block motion. The block gradually loses energy and speed until it stops. This process is related to the interaction between the block and the slope, which is realised through impacts and rebounds depending on the characteristics of the materials of the slope itself (Bourrier et al., 2012). Pfeiffer and Bowen (1989) introduced two dimensionless parameters to encapsulate the efficiency of collision between the block and slope.

The above-mentioned parameters, named tangential coefficient of restitution and normal coefficient of restitution, are crucial for simulating rock fall trajectories in computer programs.

The vegetation cover and the surface roughness determine the tangential coefficient of restitution, whereas the normal coefficient of restitution depends on the elasticity of the surface material. The resultant of both outgoing velocity vectors is the speed of the block after bouncing on the slope surface 

For these reasons, we produced a land use map (Fig. 6), derived from the combination of the aerial-photo interpretation and the outputs of field investigations performed along the scree slopes located at the bottom of the Crep Savath peak.

## A case study in the Italian Alps

S. Devoto et al.

Title Page

Abstract

Introduction

Conclusions

References

Tables

Figures



Back

Close

Full Screen / Esc

Printer-friendly Version

Interactive Discussion



Figure 6 includes also the trajectories of rockfall **simulations** carried out for Block 1, which was classified as the most dangerous boulder. Table 3 lists the values of the restitution coefficients selected for each land use class inserted in the map.

In this study, rock fall simulations were performed through a probabilistic method (Frattini et al., 2008), using two-dimensional RocFall<sup>®</sup> software (Stevens, 1998).

This computer program uses a hybrid approach (Guzzetti et al., 2002), combining a lumped mass approach for simulating free fall and a rigid body approach for simulating rolling, impact and rebound.

The step after the definition of the coefficients of restitution concerns the selection of critical 2-D cross sections along which the software simulates the rock fall trajectories (Lan et al., 2010). In our study, we defined two different sections: one obtained from the contour lines of a topographic map (CTR; scale 1 : 5000) and the other derived from a LiDAR survey. The LiDAR data were collected by a helicopter flight with an average density of 60 points m<sup>-2</sup>.

The topographic variations extracted by CTR and DTM, derived by ALS survey, are significant. In particular, the differences related to the slope angle, slope aspect and curvature generate two different rock fall trajectories (Fig. 6).

Each slice of the above-mentioned simulation **trajectories** has been divided and classified according to the land use map. The software RocFall<sup>®</sup> offers the possibility to define the slope **roughness**: a variation range of  $\pm 3^\circ$  was used on the individual segments of the section. In this way even small and undetectable topographic variations were considered and may influence the rock fall trajectories (Schweigl et al., 2003).

With regard to parameters, the rock fall computer simulations require as accurate as possible input data (Salvini et al., 2013). For this reason, we used the values reported in the literature (Stevens, 1998; Barbero and Barla, 2006) or tested in rock fall simulations performed in zones situated near Cimolais, such as western Friuli (Marussich, 2007) or the Alto Adige Region (Boccali, 2007; Piacentini and Soldati, 2008).

The simulations assume that the detachment of the loose boulders occurs on the highest outcrops of the sections in question (Figs. 7 and 8), corresponding to the po-

A case study in the Italian Alps

S. Devoto et al.

Title Page

Abstract

Introduction

Conclusions

References

Tables

Figures



Back

Close

Full Screen / Esc

Printer-friendly Version

Interactive Discussion



sition of Block 1 (Fig. 2). The mass of this boulder was calculated from the estimated volume (Table 4) and multiplied by the density of Vajont Limestone ( $2.7 \text{ g cm}^{-3}$ ). According to Barbero and Barla (2006), we set up the initial velocity at 0 and  $1.5 \text{ m s}^{-1}$  in the vertical and horizontal directions, respectively, to simulate a possible expulsion of the block because of seismic acceleration.

As the tutorial of RocFall<sup>®</sup> suggests, the initial angular velocity is set to zero. The program also allows the simulated rocks to rotate during travel by using the “consider angular velocity” checkbox. Most rocks start with little angular movement; however, during their travel down the slope, these rocks can start rotating quickly.

The computer program also envisages the adoption of correction parameters to the normal restitution coefficient (“Scale Rn by velocity” checkbox). The concept behind scaling the normal coefficient of restitution by the velocity is that Rn is not independent of velocity. For example, at low speeds, a block may bounce on grass, whereas at higher speeds, the block may imbed further into the ground before rebounding, or start to break. In these cases, the effective value of Rn should be less at higher velocities. The program uses the equation established by Pfeiffer and Bowen (1989) to calculate the scaling factor and the scaled Rn.

## 5.2 Rock fall simulation outputs

Figures 7 and 8 associate the block trajectories outputs to the morphological and land use variations along the two slopes derived by CTR map and ALS DTM, respectively.

The numerical simulations enabled the definition, in a precise way, of the boulder deposition areas, the heights of the blocks and the kinetic energy of the boulders along the entire sections.

Figure 7 shows the CTR derived section with the simulated rock fall paths. In total, 80% of the samples stop within the vegetated talus, located northerly with respect to Cimolais. However, a portion of the simulated blocks can threaten the infrastructure and people located in the northern part of Cimolais.

## A case study in the Italian Alps

S. Devoto et al.

Title Page

Abstract

Introduction

Conclusions

References

Tables

Figures

◀

▶

◀

▶

Back

Close

Full Screen / Esc

Printer-friendly Version

Interactive Discussion



## A case study in the Italian Alps

S. Devoto et al.

Title Page

Abstract

Introduction

Conclusions

References

Tables

Figures

◀

▶

◀

▶

Back

Close

Full Screen / Esc

Printer-friendly Version

Interactive Discussion



As illustrated in Figs. 7 and 9, the blocks bounce (with heights exceeding 40 m) at the second bedrock outcrop (at 900 m a.s.l.) and then, within 50 m along the horizontal, gradually pass to a rolling motion along the debris with the almost total minimization of the bouncing heights. A net decrease of the kinetic energy highlights the slowing down of the blocks. Only a small part of the 1000 boulders preserve the energy required to reach northern part of Cimolais Village.

Conversely, along the trajectory determined by the ALS survey, all of the simulated blocks arrest to the north of Cimolais Village. These results can be attributed to the final slope sector, which is characterised by a gentle gradient compared to the CTR slope and by the presence of several ledges detected in the LiDAR survey. For these reasons, the energy and speed of the boulders decrease and vanish before reaching Cimolais Village (Fig. 10).

In both cases, the volume of the boulders implies high kinetic energies. Fortunately, simulation outputs show the progressive reduction of this energy related to the long path that characterised the entire vegetated mountainside upstream of Cimolais.

## 6 Discussion

The simulated scenarios partially confirm the high rock fall risk for the northern buildings of Cimolais Village. In the CTR section, approximately 20 % of the boulders reach the urban area. The presence of the large debris cone with abundant deposits contributes to a net reduction of the high energy acquired by blocks falling by the top of Crep Savath slab, limiting their rolling motions.

Guzzetti et al. (2003) observed that talus deposits and debris cones decreases the frequency of occurrence of rock falls with increasing distance from the base of the rock fall source. Through field inspections of past rock falls, above-cited authors indicated that boulders travel mostly on the ground (i.e. rolling) or very close to the ground at low or very low velocities in the final portion of travels, similar to the final sector of simulation performed along the ALS-derived slope.

Despite the simulation outputs, local authorities cannot undervalue the rock fall hazard (Salvati et al., 2014), considering the possible presence of ground accelerations related to the frequent occurrence of earthquakes.

Furthermore, the substantial volume of unstable blocks and their high kinetic energy associated with the falling phase have to motivate authorities to adopt proper mitigation works to reduce the residual landslide risk.

Notably with regard to the results of the simulations along the two sections, rock fall barriers located between Cimolais Village and the Crep Savath slab are absent (ALS-derived trajectory) or completely inadequate to stop the block kinetic energies achieved from the simulations (CTR-derived trajectory).

To arrest or partially contain falling blocks, some of which could be fragmented during motion and terrain impacts, rock fall barriers with 5000 kJ energy absorption capacities have to be installed properly.

Figure 11 illustrates possible locations of new fences, according to simulation outputs along the two trajectories.

## 7 Conclusions

The outcomes of geomorphological field investigations performed on top of the Crep Savath slab and its surroundings recognised several unstable blocks that can affect the Fesena Valley or reach the buildings situated on the northern portion of the Cimolais Village (NE Italy).

The position of a 420 m<sup>3</sup> block and the high-angle of the slopes located between Cimolais Village and the structural escarpment, which limits the Crep Savath slab, generate a potentially highly hazardous situation for Cimolais inhabitants. This risk is historically known by local populations and is witnessed through oral tradition: the stability of the most hazardous block is related to an invisible wire mounted by an old witch.

## A case study in the Italian Alps

S. Devoto et al.

Title Page

Abstract

Introduction

Conclusions

References

Tables

Figures

◀

▶

◀

▶

Back

Close

Full Screen / Esc

Printer-friendly Version

Interactive Discussion





## A case study in the Italian Alps

S. Devoto et al.

Title Page	
Abstract	Introduction
Conclusions	References
Tables	Figures
◀	▶
◀	▶
Back	Close
Full Screen / Esc	
Printer-friendly Version	
Interactive Discussion	



Particular attention was devoted to the identification of a direct relationship between slope-failure **activities** and external triggering factors because the eastern sector of Italian Alps is located in a tectonically active zone and is characterised by annual rainfalls often exceeding 2000 mm year<sup>-1</sup>. Nevertheless, the lack of detailed landslide inventories in the NW Friuli hinders the identification of a clear correlation between predisposing factors and rock falls, although the relationship is probable and evident.

Two-dimensional simulations were performed using a hybrid computer program along two rock fall trajectories determined by contour lines derived by regional topography and by an ALS survey. The areas of potential run-out of blocks confirmed the hazardous situation, although the computer outputs recognised possible interactions between 20 % of blocks detached from the Crep Savath slab and Cimolais Village only along the slope determined by regional topography.

For this reason, urgent operations are required for civil protection and have to be performed contemporarily on the transit areas and on the rock fall source zone. Block 1 requires the installation of rock fall barriers with 5000 kJ energy absorption capacities, whereas also active mitigation measures have to be operated on the top of the Crep Savath slab. To reduce the landslide hazard, we suggest anchoring Block 1 laterally to intact limestone masses or alternatively installing an automated fissurimeter connected to an early-warning device. Aperture variations of fractures, which isolate the background of the Block 1, can activate alarm signals connected directly to the Regional Geological Survey head offices or civil protection operators.

*Acknowledgements.* The authors are grateful to Lara Tiberi (University of Trieste) for assisting in the collection and analysis of earthquake inventories.

### References

Agliardi, F., Crosta, G. B., and Frattini, P.: Integrating rockfall risk assessment and counter-measure design by 3D modelling techniques, Nat. Hazards Earth Syst. Sci., 9, 1059–1073, doi:10.5194/nhess-9-1059-2009, 2009.

## A case study in the Italian Alps

S. Devoto et al.

Title Page

Abstract

Introduction

Conclusions

References

Tables

Figures

◀

▶

◀

▶

Back

Close

Full Screen / Esc

Printer-friendly Version

Interactive Discussion



- Barbero, M. and Barla, G.: Analisi di stabilità in condizioni statiche e dinamiche di una parete rocciosa allo sbocco di una galleria autostradale: la Rocca di S. Ambrogio in Sicilia, in: Proceedings of XI Ciclo di Conferenze di Meccanica e Ingegneria delle Rocce, Torino, Italy, November 2006, 305–321, 2006.
- 5 Boccali, C.: Applicazione di software di simulazione per l'analisi di fenomeni franosi di crollo: casi di studio in Val Gardena (Provincia di Bolzano, Italia), BS thesis, University of Trieste, Trieste, Italy, 2007.
- Bourrier, F., Berger, F., Tardif, P., Dorren, L. K. A., and Hungr, O.: Rockfall rebound: comparison of detailed field experiments and alternative modelling approaches, *Earth Surf. Proc. Land.*, 37, 656–665, 2012.
- 10 Bruschi, A.: *Meccanica delle Rocce*, Dario Flaccovio Editore, Firenze, 2004.
- Cavallin, A., Sterlacchini, S., Frigerio, I., and Frigerio, S.: GIS techniques and decision support system to reduce landslide risk: the case of study of Corvara in Badia, northern Italy, *Geogr. Fis. Din. Quat.*, 34, 81–88, 2011.
- 15 Carulli, G. B.: *Carta Geologica del Friuli Venezia Giulia*, S.El.Ca, Firenze, 2006.
- Chiarabba, C., Jovane, L., and DiStefano, R.: A new view of Italian seismicity using 20 years of instrumental recordings, *Tectonophysics*, 395, 251–268, 2005.
- Cocco, S.: Definizione dei coefficienti di dissipazione dell'energia, *Acta Geol.*, 68, 3–30, 1993.
- 20 Crosta, G. B.: Regionalization of rainfall thresholds: an aid to landslide hazard evaluation, *Environ. Geol.*, 35, 131–145, 1998.
- Crosta, G. B. and Agliardi, F.: A methodology for physically based rockfall hazard assessment, *Nat. Hazards Earth Syst. Sci.*, 3, 407–422, doi:10.5194/nhess-3-407-2003, 2003.
- Cruden, D. M. and Varnes, D. J.: Landslide types and processes, in: *Landslides: Investigation and Mitigation*, edited by: Turner, A. K. and Schuster, R. L., Transportation Res. Board, Special Report 247, National Academy Press, Washington DC, 36–75, 1996.
- 25 Del Maschio, L., Gozza, G., Piacentini, D., Pizziolo, M., and Soldati, M.: Previsione delle traiettorie di blocchi mobilizzati da frane di crollo: applicazione e confronto di modelli, *Giornale di Geologia Applicata*, 6, 33–44, 2007.
- Dorren, L. K. A.: A review of rockfall mechanics and modelling approaches, *Prog. Phys. Geog.*, 27, 69–87, 2003.
- 30 Duman, T. Y., Can, T., Emre, Ö., Kecer, M., Doğan, A., Ates, S., and Durmaz, S.: Landslide inventory of northwestern Anatolia, Turkey, *Eng. Geol.*, 77, 99–114, 2005.

## A case study in the Italian Alps

S. Devoto et al.

Title Page

Abstract

Introduction

Conclusions

References

Tables

Figures

◀

▶

◀

▶

Back

Close

Full Screen / Esc

Printer-friendly Version

Interactive Discussion



Dykes, A. P., Bromhead, E. N., Hosseyni, S. M., and Ibsen, M.: A geomorphological reconnaissance of structurally-controlled landslides in the Dolomites, Italian J. Eng. Geol. Environ., 6, 133–140, 2013.

Fazzini, M.: Definizione quantitativa dei regimi pluviometrici nelle Alpi orientali italiane – a new method to quantitatively discriminate the pluviometric regimes of the Eastern Italian Alps, in: Proceedings of the Conferences “Mountains and Plains”, Padova, Italy, 15–17 February 2005, Geogr. Fis. Din. Quat., VII, 155–162, 2005.

Flageollet, J. C. and Weber, D.: Fall, in: Landslides Recognition: Identification, Movement and Courses, edited by: Dikau, R., Brunsden, D., Schrott, L., and Ibsen, M. L., Wiley, Chichester, England, 13–28, 1996.

Fratini, P., Crosta, G. B., Carrara, A., and Agliardi, F.: Assessment of rockfall susceptibility by integrating statistical and physically-based approaches, Geomorphology, 94, 419–437, 2008.

Govi, M.: Photo-interpretation and mapping of the landslides triggered by the Friuli earthquake (1976), B. Int. Assoc. Eng. Geol., 15, 67–72, 1977.

Guzzetti, F.: Landslide fatalities and the evaluation of landslide risk in Italy, Eng. Geol., 58, 89–107, 2000.

Guzzetti, F., Crosta, G. B., Detti, R., and Agliardi, F.: STONE: a computer program for the three-dimensional simulation of rock-falls, Comput. Geosci., 28, 1079–1093, 2002.

Guzzetti, F., Reichenbach, P., and Wieczorek, G. F.: Rockfall hazard and risk assessment in the Yosemite Valley, California, USA, Nat. Hazards Earth Syst. Sci., 3, 491–503, doi:10.5194/nhess-3-491-2003, 2003.

Hack, R., Alkema, D., Kruse, G. A. M., Leenders, N., and Luzi, L.: Influence of earthquakes on the stability of slopes, Eng. Geol., 91, 4–15, 2007.

INGV: Italian Seismological Instrumental and Parametric Database, available at: <http://iside.rm.ingv.it> (last access: September, 2014), 2010.

Jibson, R. W. and Keefer, D. K.: Statistical analysis of factors affecting landslide distribution in the New Madrid seismic zone, Tennessee and Kentucky, Eng. Geol., 27, 509–542, 1989.

Keefer, D. K.: Landslides caused by earthquakes, Geol. Soc. Am. Bull., 95, 406–421, 1984.

Keefer, D. K.: Investigating landslides caused by earthquakes – a historical review, Surv. Geophys., 23, 473–510, 2002.

Köppen, W.: Grundriss de Klimakunde, 2nd Edn., W. De Gruyter, Berlin, 1931.

**A case study in the Italian Alps**

S. Devoto et al.

Title Page

Abstract

Introduction

Conclusions

References

Tables

Figures

I◀

▶I

◀

▶

Back

Close

Full Screen / Esc

Printer-friendly Version

Interactive Discussion



Krautblatter, M. and Moser, M.: A nonlinear model coupling rockfall and rainfall intensity based on a four year measurement in a high Alpine rock wall (Reintal, German Alps), *Nat. Hazards Earth Syst. Sci.*, 9, 1425–1432, doi:10.5194/nhess-9-1425-2009, 2009.

Lan, H., Martin, C. D., Zhou, C., and Lim, C. H.: Rockfall hazard analysis using LiDAR and spatial modeling, *Geomorphology*, 118, 213–223, 2010.

Marcato, G., Mantovani, M., Pasuto, A., Silvano, S., Tagliavini, F., Zabuski, L., and Zannoni, A.: Site investigation and modelling at “La Maina” landslide (Carnian Alps, Italy), *Nat. Hazards Earth Syst. Sci.*, 6, 33–39, doi:10.5194/nhess-6-33-2006, 2006.

Martinis, B.: Studio geologico dell’area maggiormente colpita dal terremoto friulano del 1976, Consiglio Nazionale delle Ricerche, Comitato per le Scienze Geologiche e Minerarie, Progetto Finalizzato Geodinamica, Milano, 201–393, 1977.

Marussich, D.: Valutazione della Pericolosità e Analisi del Rischio da Crolli in Località Frasen (Comune di Erto e Casso), BS thesis, University of Trieste, Trieste, Italy, 2007.

Matsuoka, N. and Sakai, H.: Rockfall activity from an alpine cliff during thawing periods, *Geomorphology*, 28, 309–328, 1999.

McCauley, M. L., Works, B. W., and Naramore, S. A.: Rockfall Mitigation, Report FHWA/CA/TL-85/12, FHWA, US Department of Transportation, California, 1985.

Mignelli, C., Peila, D., Lo Russo, S., Ratto, S. M., and Broccolato, M.: Analysis of rockfall risk on mountainside roads: evaluation of the effects of protection devices, *Nat. Hazards*, 73, 23–35, 2014.

Onofri, R. and Candian, C.: Indagine sui Limiti di Massima Invasione dei Blocchi Rocciosi Frantati Durante il Sisma del Friuli del 1976, Regione Autonoma Friuli-Venezia Giulia, CLUET, Trieste, Italy, 1979.

Panizza, M.: The Geomorphology of the Dolomites from a geomorphodiversity viewpoint, *Geogr. Fis. Din. Quat.*, 34, 25–32, 2011.

Parise, M.: Landslide hazard zonation of slopes susceptible to rock falls and topples, *Nat. Hazards Earth Syst. Sci.*, 2, 37–49, doi:10.5194/nhess-2-37-2002, 2002.

Paronuzzi, P.: La fragilità idrogeologica dell’ambiente montano, in: *Il Tagliamento*, edited by: Bianco, F., Bondesan, A., Zanetti, M., and Zanferrari, A., Cierre Edizioni, Caselle di Sommacampagna, Verona, Italy, 99–109, 2006.

Paronuzzi, P. and Gnech, D.: Frane di crollo indotte da piogge intense: la casistica del Friuli-Venezia Giulia (Italia NE), *Giornale di Geologia Applicata*, 6, 55–64, 2007.

## A case study in the Italian Alps

S. Devoto et al.

Title Page

Abstract

Introduction

Conclusions

References

Tables

Figures

◀

▶

◀

▶

Back

Close

Full Screen / Esc

Printer-friendly Version

Interactive Discussion



- Pfeiffer, T. J. and Bowen, T. D.: Computer simulation of rockfalls, *B. Assoc. Eng. Geol.*, 26, 135–146, 1989.
- Piacentini, D. and Soldati, M.: Application of empiric models for the analysis of rock-fall runout at a regional scale in mountain areas: examples from the Dolomites and the northern Apennines (Italy), *Geogr. Fis. Din. Quat.*, 31, 215–223, 2008.
- Piacentini, T., Miccadei, E., Di Michele, R., Sciarra, N., and Mataloni, G.: Geomorphological analysis applied to rock falls in Italy: the case of the San Venanzio Gorges (Aterno River, Abruzzo, Italy), *Italian J. Eng. Geol.*, 6, 467–479, 2013.
- Riva, M., Besio, M., Masetti, D., Roccati, F., Sapigni, M., and Semenza, E.: *Geologia delle Valli Vajont e Gallina (Dolomiti Orientali)*, *Ann. Univ. Ferrara*, 2, 55–76, 1990.
- Rocscience Inc.: *Rocfall User's Guide*, Toronto, Canada, 1998.
- Rogers, T. H. and Cluff, L. S.: The May 1976 Friuli earthquake (Northeastern Italy) and interpretations of past and future seismicity, *Tectonophysics*, 52, 521–532, 1979.
- Salvati, P., Bianchi, C., Fiorucci, F., Giostrella, P., Marchesini, I., and Guzzetti, F.: Perception of flood and landslide risk in Italy: a preliminary analysis, *Nat. Hazards Earth Syst. Sci.*, 14, 2589–2603, doi:10.5194/nhess-14-2589-2014, 2014.
- Salvini, R., Francioni, M., Riccucci S., Fantozzi, P.L., Bonciani, F., and Mancini, S.: Stability analysis of “Grotta delle Felci” Cliff (Capri Island, Italy): structural, engineering-geological, photogrammetric surveys and laser scanning, *B Eng. Geol. Environ.*, 70, 549–557, 2011.
- Salvini, R., Francioni, M., Riccucci, S., Bonciani, F., and Callegari, I.: Photogrammetry and laser scanning for analyzing slope stability and rock fall runout along the Domodossola-Iselle railway, the Italian Alps, *Geomorphology*, 185, 110–122, 2013.
- Schweigl, J., Ferretti, C., and Nössing, L.: Geotechnical characterization and rockfall simulation of a slope: a practical case study from South Tyrol (Italy), *Eng. Geol.*, 67, 281–296, 2003.
- Sidle, R. C. and Ochiai, H.: *Landslides: Processes, Prediction, and Land Use*, *Water Res. M.*, Washington, 312 pp., 2006.
- Stevens, W.: *Rocfall: a Tool for Probabilistic Analysis, Design of Remedial Measures and Prediction of Rock Falls*, MS thesis, University of Toronto, Canada, 1998.
- Tagliavini, F., Reichenbach, P., Maragna, D., Guzzetti, F., and Pasuto, A.: Comparison of 2-D and 3-D computer models for the M. Salta rock fall, Vajont Valley, northern Italy, *Geoinformatica*, 13, 323–337, 2009.
- Valagussa, A., Frattini, P., and Crosta G. B.: Earthquake-induced rockfall hazard zoning, *Eng. Geol.*, 182, 213–225, 2014.

Wieczorek, G. F. and Jäger, S.: Triggering mechanisms and depositional rates of postglacial slope-movement processes in the Yosemite Valley, California, *Geomorphology*, 15, 17–31, 1996.

# NHESSD

2, 7329–7365, 2014

## A case study in the Italian Alps

S. Devoto et al.

Title Page

Abstract

Introduction

Conclusions

References

Tables

Figures



Back

Close

Full Screen / Esc

Printer-friendly Version

Interactive Discussion



## A case study in the Italian Alps

S. Devoto et al.

**Table 1.** Main properties of unstable boulders.

Block	Volume [m <sup>3</sup> ]	Direction	Rock-fall susceptibility
Block 1	420	Cimolais Village	Extremely high
Block 2	18	Cimolais Village	Extremely high
Block 3	9	Cimolais Village	Extremely high
Block 4	24	Cimolais Village	Extremely high
Block 5	6	Cimolais Village	Extremely high
Block 6	6	Fesena Valley	Low
Block 7	2	Fesena Valley	Fair
Block 8	12	Fesena Valley	Fair
Block 9	126	Fesena Valley	High
Block 10	1	Fesena Valley	High
Block 11	6	Fesena Valley	Fair
Block 12	5	Fesena Valley	Low
Block 13	1	Fesena Valley	Low

[Title Page](#)
[Abstract](#)
[Introduction](#)
[Conclusions](#)
[References](#)
[Tables](#)
[Figures](#)

[Back](#)
[Close](#)
[Full Screen / Esc](#)
[Printer-friendly Version](#)
[Interactive Discussion](#)


**Table 2.** Historical earthquakes within 250 km of Cimolais with  $M > 5.4$ . Source: Italian Seismological and parametric database, INGV (2010).

Date	Zone of maximum effects	Magnitude
28 Jul 1700	Raveo (Friuli, Italy)	5.7
12 Jan 1721	Rijeka (Croazia)	6.0
10 Jul 1776	Tramonti (Friuli, Italy)	5.8
4 Apr 1781	Faentino (Italy)	5.8
20 Oct 1788	Tolmezzo (Friuli, Italy)	5.8
22 Oct 1796	Eastern Emilia (Italy)	5.6
12 May 1802	Valle dell'Oglio (Italy)	5.5
25 Oct 1812	Sequals (Friuli, Italy)	5.5
13 Mar 1832	Reggio Emilia (Italy)	5.5
30 Oct 1870	Cesena County (Italy)	5.4
29 Jun 1873	Belluno County (Italy)	6.3
17 Mar 1875	Cesena County (Italy)	5.6
7 Jun 1891	Verona County (Italy)	5.6
14 Apr 1895	Ljubljana (Slovenia)	6.2
30 Oct 1901	Brescia County (Italy)	5.5
9 Jan 1917	Brežice-Krška vas (Slovenia)	5.7
1 Jan 1926	Cerknica- Unec (Slovenia)	5.2
27 Mar 1928	Carnia (Friuli, Italy)	5.6
18 Oct 1936	Treviso County (Italy)	5.8
15 Jul 1971	Parma (Italy)	5.4
6 May 1976	Eastern Friuli (Italy)	6.4
11 Sep 1976	Eastern Friuli (Italy)	5.8
11 Sep 1976	Eastern Friuli (Italy)	5.6
15 Sep 1976	Eastern Friuli (Italy)	5.9
15 Sep 1976	Eastern Friuli (Italy)	6.0
12 Apr 1998	Bovec (Slovenia)	5.5
20 May 2012	Modena (Italy)	5.8
29 May 2012	Modena county (Italy)	5.6

**A case study in the Italian Alps**

S. Devoto et al.

Title Page

Abstract	Introduction
Conclusions	References
Tables	Figures
◀	▶
◀	▶
Back	Close
Full Screen / Esc	
Printer-friendly Version	
Interactive Discussion	





## A case study in the Italian Alps

S. Devoto et al.

**Table 3.** Restitution coefficients used in the simulations according to the different types of vegetation or slope materials. The right column indicates the source of the coefficients.

Slope materials	Rn	Rt	Source
Clean hard bedrock	$0.53 \pm 0.04$	$0.99 \pm 0.04$	Rocfall user's guide (1998)
Talus with vegetation	$0.32 \pm 0.04$	$0.80 \pm 0.04$	Rocfall user's guide (1998)
Asphalt/urban areas	$0.40 \pm 0.04$	$0.90 \pm 0.04$	Rocfall user's guide (1998)
Lawn	0.25	0.55	Bruschi (2004)
Forest	0.3	0.8	Piacentini et al. (2008)

Title Page

Abstract

Introduction

Conclusions

References

Tables

Figures

◀

▶

◀

▶

Back

Close

Full Screen / Esc

Printer-friendly Version

Interactive Discussion



## A case study in the Italian Alps

S. Devoto et al.

Title Page

Abstract

Introduction

Conclusions

References

Tables

Figures

◀

▶

◀

▶

Back

Close

Full Screen / Esc

Printer-friendly Version

Interactive Discussion



**Table 4.** Input parameters selected for computer simulations.

Parameter	Value	Notes
Horizontal velocity	1.5	$\text{ms}^{-1}$
Vertical velocity	0	$\text{ms}^{-1}$
Block mass	1134	t
Angular velocity	0	$\text{rads}^{-1}$
Number of rocks to throw	1000	
Minimum velocity cut off	0.1	$\text{ms}^{-1}$

## A case study in the Italian Alps

S. Devoto et al.

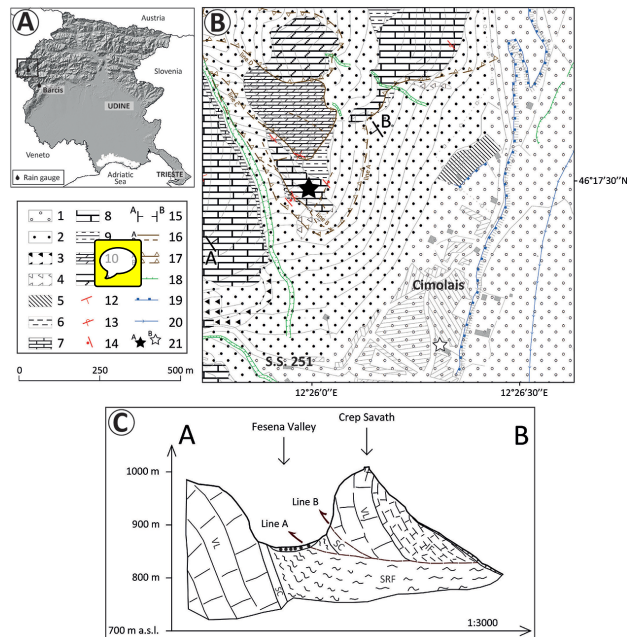


**Figure 1.** Study area: (a) Friuli Venezia Giulia region and location of rain gauges; (b) Geological map showing distribution of main lithology, major structural and geomorphological features. The legend symbols are accompanied to numbers which indicate: 1, Alluvial deposits; 2, Talus; 3, Rockfall active deposits; 4, Rockfall inactive deposits; 5, Anthropic reshaped area; 6, Scaglia Rossa Friulana Fm. (marls and reddish limestone); 7, Successione condensate Fm. (cherty limestone); 8, Vajont Limestone Fm.; 9, Igne Fm. (marls and red nodular limestone); 10, Soverzene Fm. (cherty dolostone); 11, Dolomia Principale (grey massive dolostone); 12, Attitude of the strata; 13, Reversed strata; 14, Vertical strata; 15, Trace of the geological section; 16A, Fault; 16B, Buried fault; 17A, Observed thrust; 17B, Inferred thrust; 18, Edge of fluvial erosion; 19, Edge of terrace; 20, Stream; 21A, Crep Savath; 21B, Cimolais steeple; (c) Geological section.

## A case study in the Italian Alps

S. Devoto et al.



**Figure 2.** Panoramic view of Cimolais Village and overlying Crep Savath peak (a). The red circle indicates the rock fall source areas. The oblique view from Fesena Valley (b) and the frontal view (c) highlight the hazardous position and the large dimensions of Block 1.

Title Page	
Abstract	Introduction
Conclusions	References
Tables	Figures
◀	▶
◀	▶
Back	Close
Full Screen / Esc	
Printer-friendly Version	
Interactive Discussion	



**A case study in the Italian Alps**

S. Devoto et al.

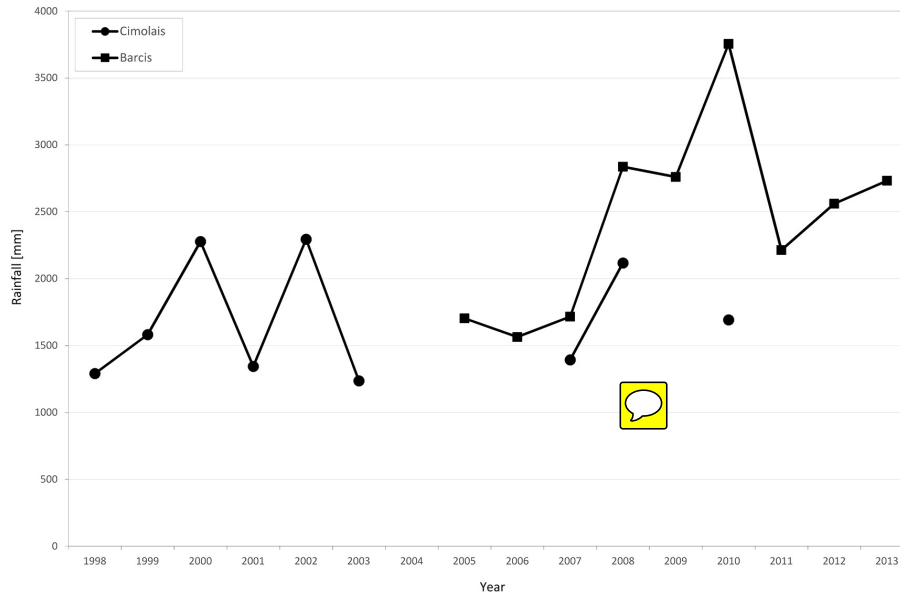


**Figure 3.** Trend of annual rainfall from 1998 to 2013, data of 2004 are missing (source: Cimolais and Barcis rain gauges, Civil Defense of FVG Region).

Title Page

Abstract

Introduction

Conclusions

References

Tables

Figures

I ◀

▶ I

◀

▶

Back

Close

Full Screen / Esc

Printer-friendly Version

Interactive Discussion



## A case study in the Italian Alps

S. Devoto et al.

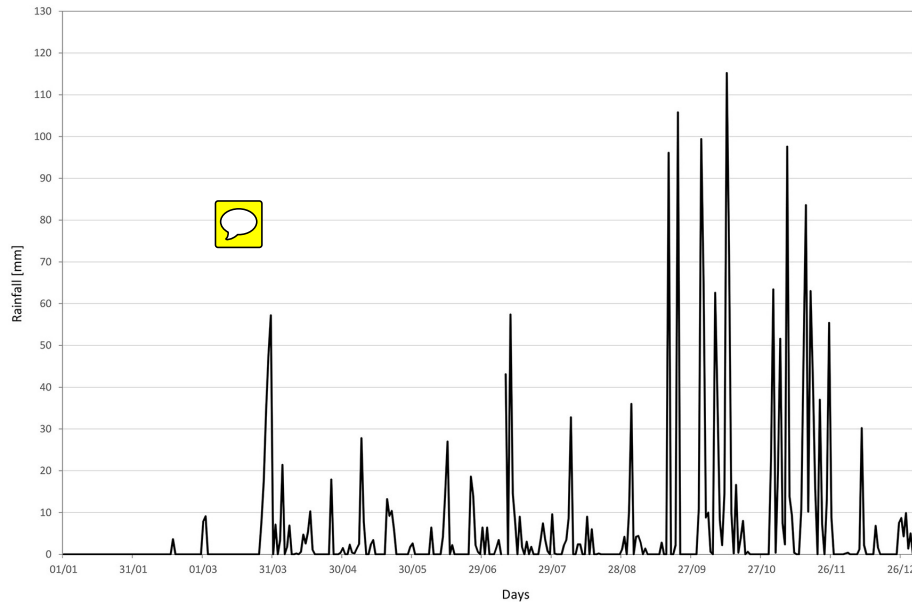


**Figure 4.** Daily precipitation occurred in 2000 (source: Cimolais rain gauge, Civil Defense of FVG Region).

Title Page	
Abstract	Introduction
Conclusions	References
Tables	Figures
◀	▶
◀	▶
Back	Close
Full Screen / Esc	
Printer-friendly Version	
Interactive Discussion	



**A case study in the Italian Alps**

S. Devoto et al.

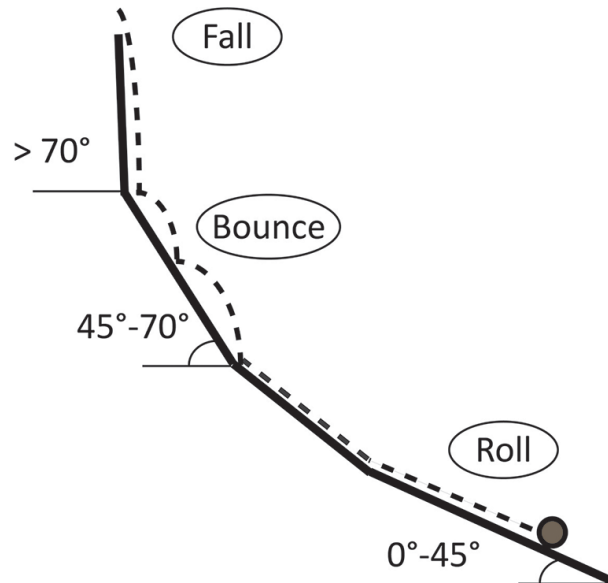


**Figure 5.** Different type of block motions related to the mean dip of slope (modified from Dorren, 2003).

Title Page

Abstract

Introduction

Conclusions

References

Tables

Figures

◀

▶

◀

▶

Back

Close

Full Screen / Esc

Printer-friendly Version

Interactive Discussion



## A case study in the Italian Alps

S. Devoto et al.

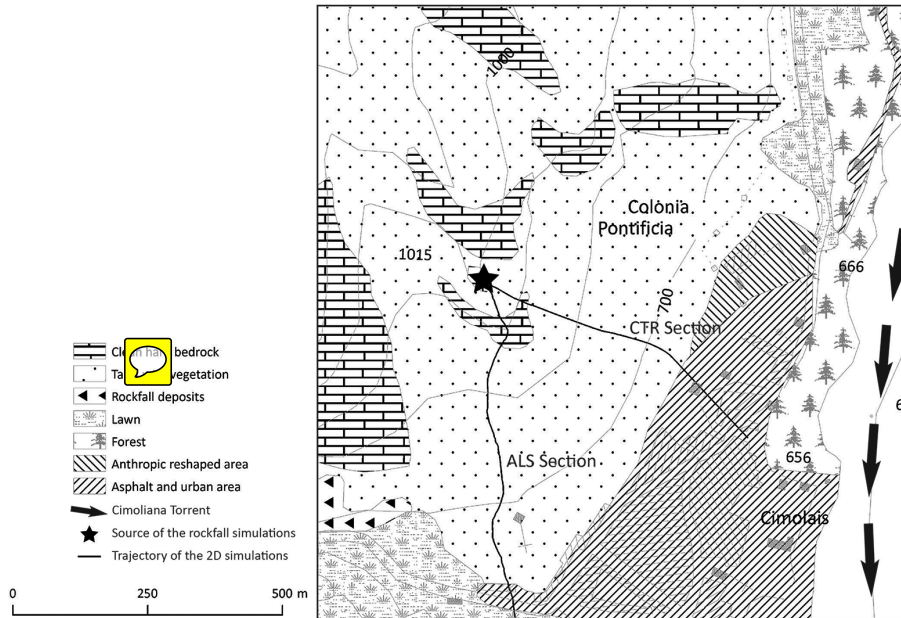


**Figure 6.** Land use map including the source area of rock falls and simulation trajectories.

Title Page

Abstract

Introduction

Conclusions

References

Tables

Figures

◀

▶

◀

▶

Back

Close

Full Screen / Esc

Printer-friendly Version

Interactive Discussion





## A case study in the Italian Alps

S. Devoto et al.

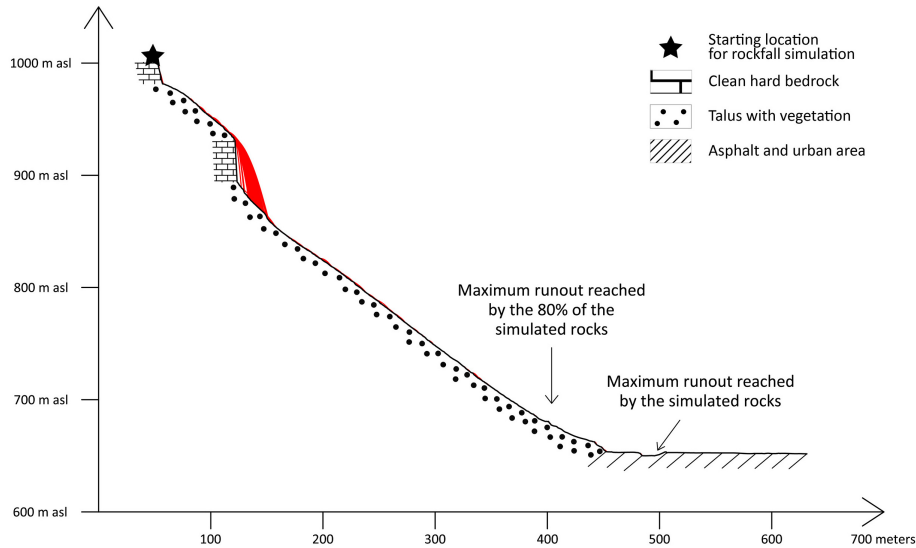


**Figure 7.** Rock fall trajectories simulated along the CTR-derived profile.

Title Page	
Abstract	Introduction
Conclusions	References
Tables	Figures
◀	▶
◀	▶
Back	Close
Full Screen / Esc	
Printer-friendly Version	
Interactive Discussion	



## A case study in the Italian Alps

S. Devoto et al.

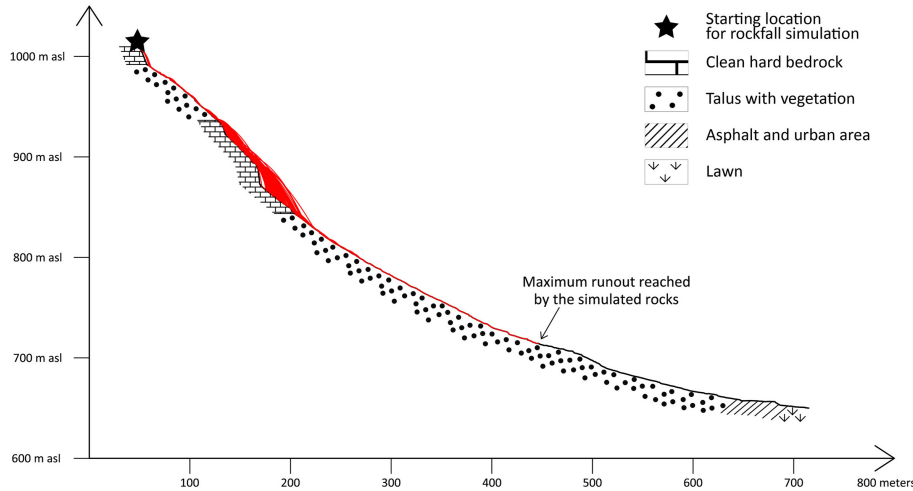


**Figure 8.** Rock fall trajectories simulated along slope implemented by means of an ALS-derived DTM.

Title Page

Abstract

Introduction

Conclusions

References

Tables

Figures

◀

▶

◀

▶

Back

Close

Full Screen / Esc

Printer-friendly Version

Interactive Discussion



## A case study in the Italian Alps

S. Devoto et al.

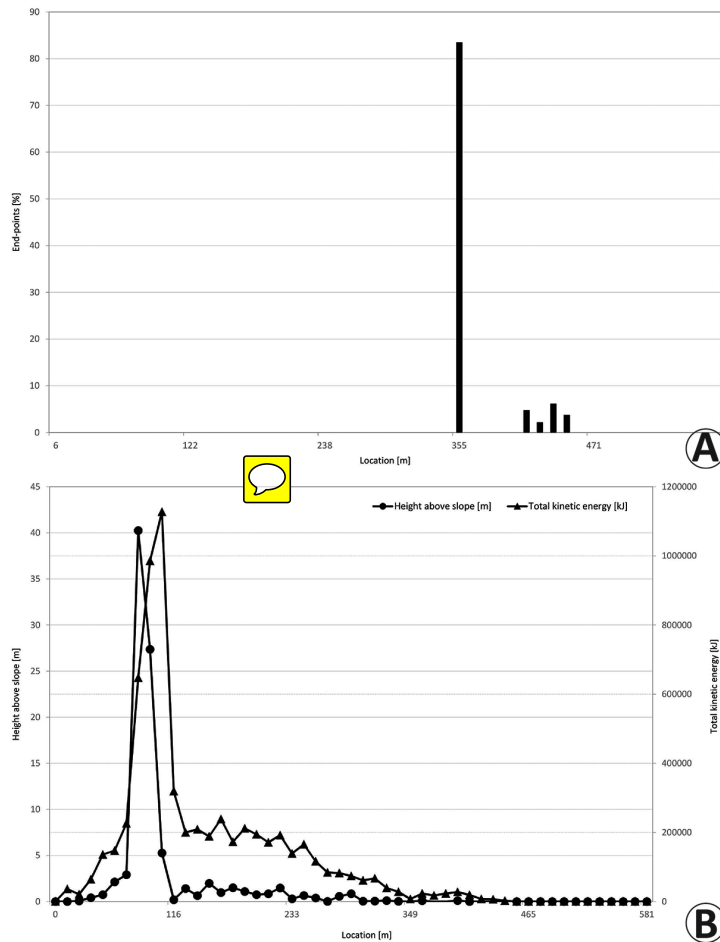


**Figure 9.** Blocks run-out (a), bounce heights and kinetic energy distributions (b) along the CTR-derived profile.



## A case study in the Italian Alps

S. Devoto et al.

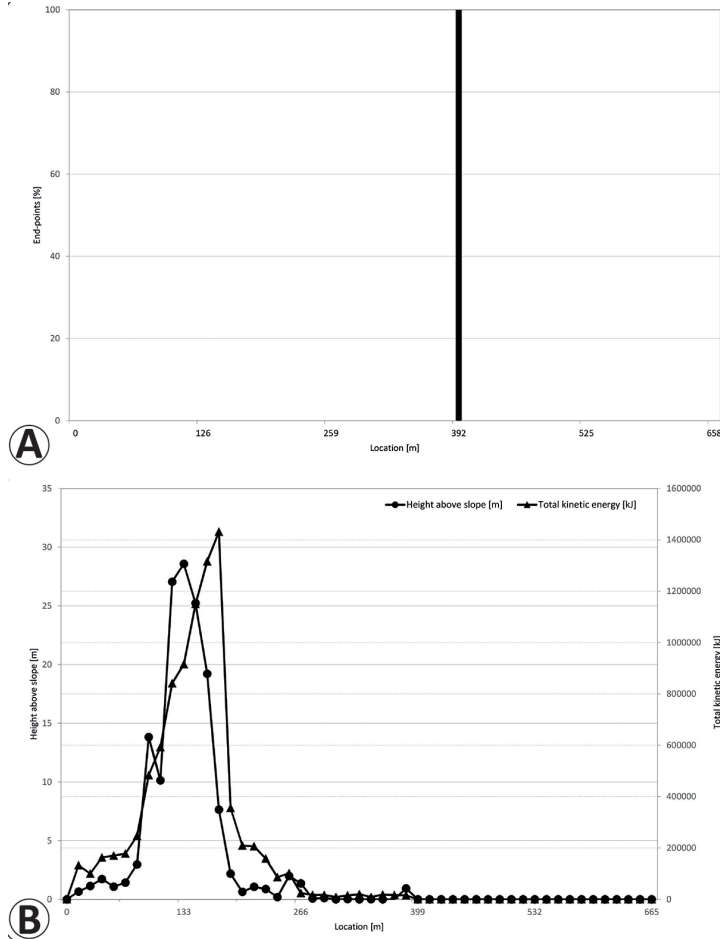


**Figure 10.** Blocks run-out **(a)**, bounce heights and kinetic energy distributions **(b)** along the ALS-derived profile.

Title Page

Abstract	Introduction
Conclusions	References
Tables	Figures

⏪
⏩

◀
▶

Back
Close

Full Screen / Esc

Printer-friendly Version

Interactive Discussion



## A case study in the Italian Alps

S. Devoto et al.

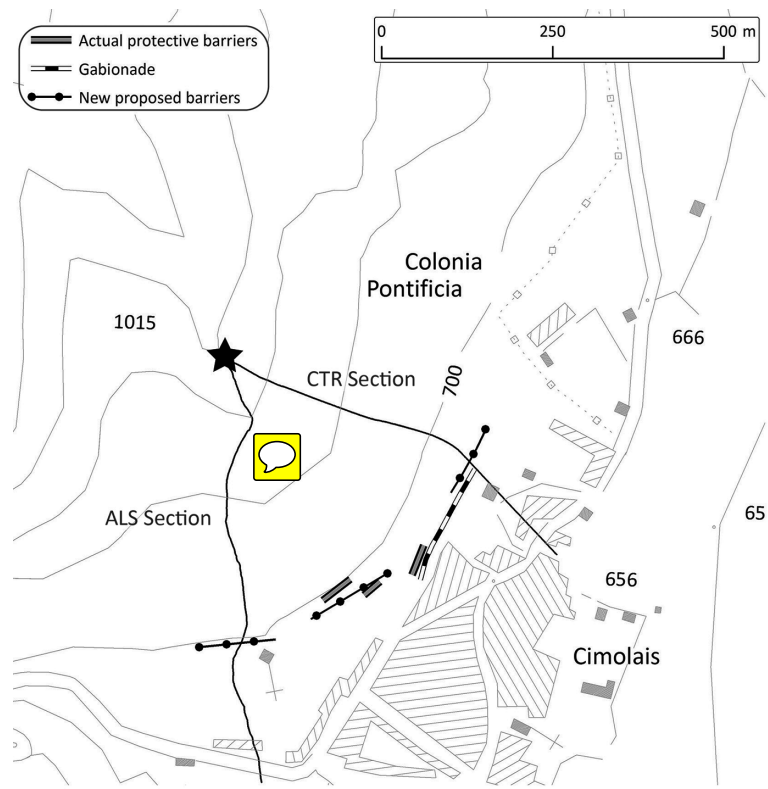


**Figure 11.** Actual position of mitigation works and proposed location of new barriers.

Title Page	
Abstract	Introduction
Conclusions	References
Tables	Figures
◀	▶
◀	▶
Back	Close
Full Screen / Esc	
Printer-friendly Version	
Interactive Discussion	

